

HIGH DIELECTRIC SHEET TO REDUCE ELECTRIC FIELDS AND FLATTEN MAGNETIC FIELDS IN SELF-DECOUPLED RADIOFREQUENCY COILS FOR MR IMAGING

Aditya Bhosale¹, Xiaoliang Zhang^{1,2}

¹Department of Biomedical Engineering, ²Department of Electrical Engineering, State University of New York at Buffalo, NY 14260, USA

Abstract— High impedance RF coils, such as self-decoupled coils, reduce the electromagnetic coupling between the coil elements and eliminates the use of complex decoupling technologies. Although the high impedance design promises excellent decoupling between the coil elements, it also results in high electric fields across the RF coil, leading to potential safety problems during imaging. It also causes B1 field asymmetry, ultimately leading to difficulties in imaging quantification. In this study, we propose and investigate using a high dielectric sheet to reduce the electric fields across the coil and achieve excellent electromagnetic decoupling among the coil elements, thereby ensuring safer MRI at ultra-high fields and maintaining high imaging performance.

I. INTRODUCTION

In magnetic resonance imaging, arrays of radiofrequency coils are commonly used to achieve high signal-to-noise ratios and versatile volume coverage, speed up scans with parallel reception, and reduce field nonuniformity with the parallel transmission. On the other hand, traditional coil arrays require sophisticated decoupling technologies to minimize electromagnetic coupling between coil elements, which would otherwise amplify noise and reduce transmitted strength [1-14]. Electromagnetic coupling between RF array elements has posed a daunting challenge in designing multichannel coil arrays, particularly transceiver arrays at high and ultrahigh fields [15-27].

The recently proposed self-decoupled coil is a unique alternative to standard coils. The self-decoupled coils have a simple structure and deliberate electrical impedance redistribution along the coil loop's length. Self-decoupled coils have excellent decoupling efficiency despite their coil-orientation dependence. When used to construct an array, they are resistant to coil separation, making them appealing for size adjustable and versatile coil arrays. Easy rectangular or circular loop coils with evenly spaced capacitors connected along their length are known as conventional coils.

On the other hand, the self-decoupled coil has the same structure as a traditional coil. A comparatively high impedance is located opposite the coil's feed port, causing the coil to act like a loop and a folded dipole superimposed on each other [28-30]. Due to the small value capacitance ($\sim 0.4\text{pF}$) in the self-decoupled coil, a high electric field will be generated in the area around the capacitor. This may increase the Specific Absorption Rate (SAR), resulting in an elevated tissue-heating hazard during MR imaging examinations. The high electric fields caused by the small value capacitance can be mitigated using multiple series capacitors with relatively large capacitance values. This work proposes and investigates a method using high permittivity dielectric materials to suppress the electric field around the capacitor. Due to its unique property, the radio frequency magnetic field (B1 field) is expected not to be negatively impacted.

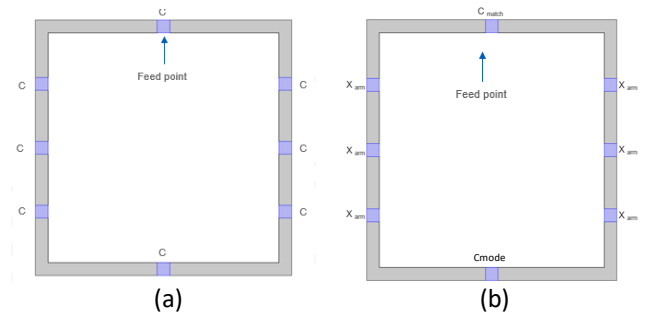


Fig. 1 (a) Conventional coil with eight capacitors (each 8 pF) spaced evenly along its length (b) Self-decoupled coil high impedance ($C_{\text{mode}}:0.44\text{pF}$) placed opposite the coil's feed port.

II. METHODS

We modeled a conventional coil, self-decoupled coil, and self-decoupled coil with a dielectric sheet. The conventional coil has eight 8pF capacitors equally distributed along its length. The self-decoupled coil comprises six X_{arm} impedances, one C_{mode} capacitor opposite the feed port, and one C_{match} capacitor to balance the self-decoupled coil's impedance. The

magnetic and electric field distribution generated through the self-decoupled coil was simulated and evaluated using a $10 \times 10 \text{ cm}^2$ self-decoupled coil. The safety concern associated with the self-decoupled coil is the higher electric fields produced across the C_{mode} capacitor of the self-decoupled coil. One method to reduce the higher electric fields produced across the coil is to break up the C_{mode} capacitor into five capacitors of 2.9pF. In this study, we propose another method that uses a high dielectric sheet to reduce the higher electric fields across the coil. We designed a $10 \times 10 \text{ cm}^2$ self-decoupled coil and mounted a 1mm thick piece of the dielectric sheet over the C_{mode} capacitor to see how the high dielectric sheet affected the electric, magnetic, and decoupling performance of the coil [13-15, 31, 32].

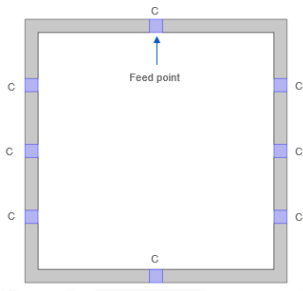


Fig. 2 Conventional coil with eight capacitors equally distributed along its length.

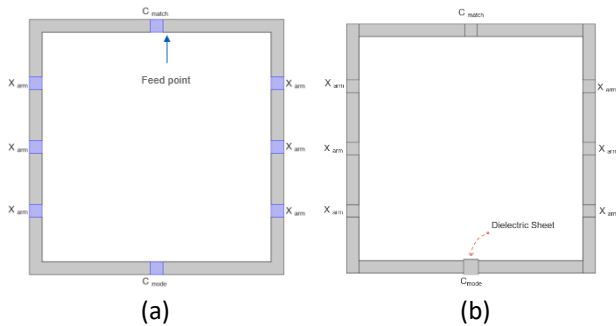


Fig. 3 (a) Self-decoupled coil (b) Dielectric sheet over C_{mode} capacitor of Self-decoupled coil.

C. High Dielectric Sheet

We placed a high dielectric sheet with a thickness of 1mm above the C_{mode} capacitor. The dimensions of the dielectric sheet were $1 \times 1 \text{ cm}^2$. The high dielectric sheet's relative permittivity was varied to test the array system's performance at different values. Figure 3 (b) shows the dielectric sheet above the self-decoupled coil.

D. Simulations

For a $10 \times 10 \text{ cm}^2$ self-decoupled coil without a dielectric layer, each X_{arm} impedance is 5.6nH & the value of the C_{mode}

capacitor is 0.44pF. The C_{match} capacitor is solely used to match the coil's impedance at 50ohm. We ran simulations with a small piece of the dielectric sheet covering the C_{mode} capacitor on the self-decoupled coil. The dielectric sheet's relative permittivity varied from 50 to 400. The resonant frequency of the self-decoupled coil was matched at 300MHz/50 ohm by tuning the X_{arm} impedances and the C_{match} capacitor to compensate for the dielectric sheet load. The self-decoupled coil's input power was kept constant at 1 Watt. The effect of the dielectric sheet on the electric fields and magnetic fields across the self-decoupled coil was observed. The decoupling efficiency was also observed using electromagnetic simulations.

E. Data Analysis

We exported the B field maps, current density plots, and S-parameters directly using COMSOL Multiphysics software. The magnetic field distribution was displayed using the following expression:

$$\text{emw.normB}$$

The surface current density plots were constructed using the following expression:

$$\text{emw.Jsurf}$$

The Electric field plots were constructed using the following expression:

$$\text{emw.normE}$$

III. RESULTS

A. Electric Field Distribution

The electric field of the conventional coil is $1.8 \times 10^3 \text{ V/m}$, while the electric field across the C_{mode} capacitor on the self-decoupled coil is $7.4 \times 10^3 \text{ V/m}$, which is almost four times higher.

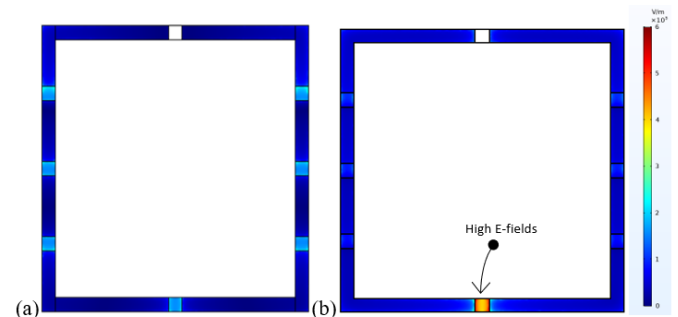


Fig. 4 Electric field distribution (a) Conventional coil (b) Self-decoupled coil

Our results show a steady decrease in the electric fields across the C_{mode} capacitor on the self-decoupled coil with a higher value of relative permittivity of the dielectric sheet. The electric field strengths across the C_{mode} capacitor for all the tested values of the dielectric sheet's relative permittivity are listed in the table below[33-37].

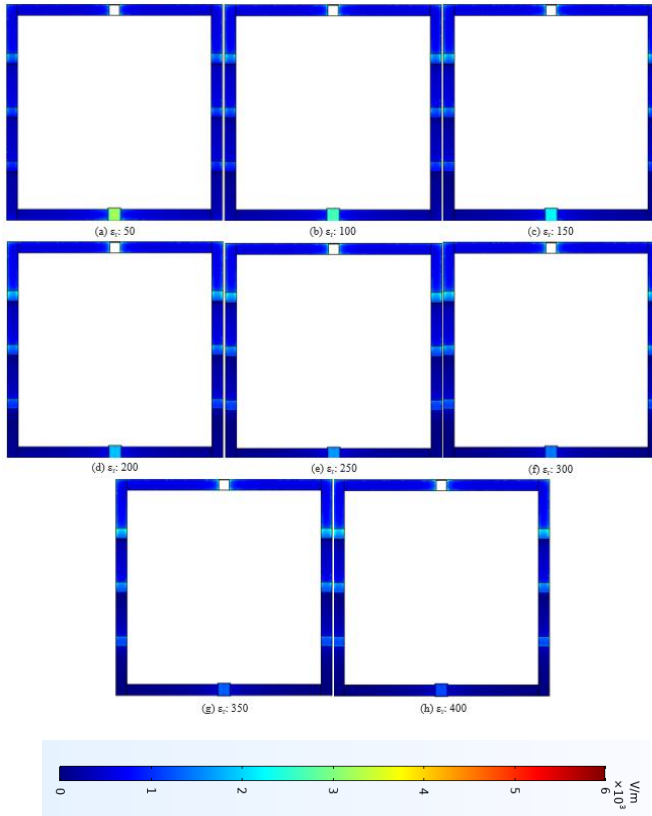


Fig. 5 Electric field distribution of a self-decoupled coil with dielectric sheet over C_{mode} capacitor (a) ϵ_r : 50 (b) ϵ_r : 100 (c) ϵ_r : 150 (d) ϵ_r : 200 (e) ϵ_r : 250 (f) ϵ_r : 300 (g) ϵ_r : 350 (h) ϵ_r : 400

Coil Type	Electric fields across C_{mode} capacitor
Self-decoupled coil without a dielectric sheet	$7.4 \times 10^3 \text{ V m}^{-1}$
Self-decoupled coil with a dielectric sheet ($\epsilon_r = 50$)	$3.2 \times 10^3 \text{ V m}^{-1}$
Self-decoupled coil with a dielectric sheet ($\epsilon_r = 100$)	$2.5 \times 10^3 \text{ V m}^{-1}$
Self-decoupled coil with a dielectric sheet ($\epsilon_r = 150$)	$2.1 \times 10^3 \text{ V m}^{-1}$
Self-decoupled coil with a dielectric sheet ($\epsilon_r = 200$)	$2 \times 10^3 \text{ V m}^{-1}$
Self-decoupled coil with a dielectric sheet ($\epsilon_r = 250$)	$1.8 \times 10^3 \text{ V m}^{-1}$
Self-decoupled coil with a dielectric sheet ($\epsilon_r = 300$)	$1.5 \times 10^3 \text{ V m}^{-1}$
Self-decoupled coil with a dielectric sheet ($\epsilon_r = 350$)	$1.2 \times 10^3 \text{ V m}^{-1}$

Self-decoupled coil with a dielectric sheet ($\epsilon_r = 400$)	$1 \times 10^3 \text{ V m}^{-1}$
--	----------------------------------

Table. 1 Effect of the dielectric sheet on electric field strength across C_{mode} capacitor on the self-decoupled coil

B. Magnetic Field Distribution

The magnetic field distributions of the conventional coil, self-decoupled coil, and self-decoupled coil with dielectric sheet are shown using the linear scale in T. The expression used is as follows: (emw.normB).

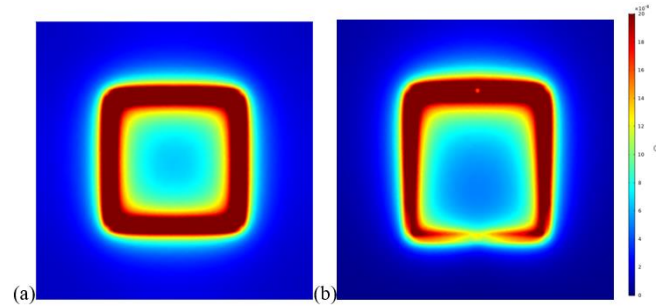


Fig. 6 Magnetic field distribution (a) Conventional coil (b) Self-decoupled coil

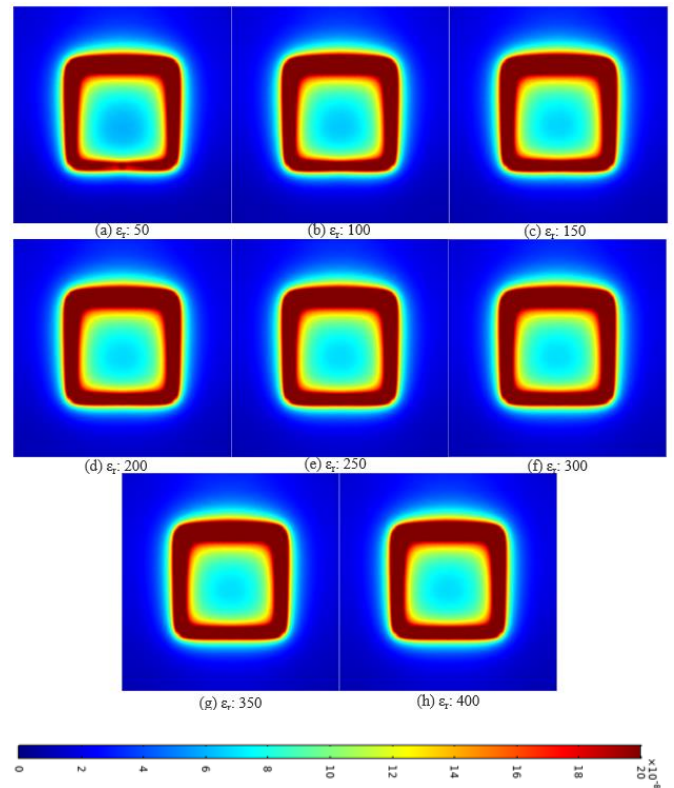


Fig. 7 Magnetic field distribution of a self-decoupled coil with dielectric sheet over C_{mode} capacitor (a) ϵ_r : 50 (b) ϵ_r : 100 (c) ϵ_r : 150 (d) ϵ_r : 200 (e) ϵ_r : 250 (f) ϵ_r : 300 (g) ϵ_r : 350 (h) ϵ_r : 400

Our findings suggest that as the relative permittivity of the dielectric layer increases, the electric fields decrease, and the magnetic field distribution becomes more uniform and balanced.

C. Decoupling Performance

The current distributions of the self-decoupled coil with the dielectric sheet on the C_{mode} capacitor are shown using the linear scale in A/m. The expression used is as follows: (emw.Jsurf). The distance between two self-decoupled coils is 1 cm. One coil is excited, while the other is kept as a passive element. The results suggest that using a high dielectric sheet does not hamper the decoupling efficiency of the self-decoupled coil, and the current induced in the passive element is negligible. Hence, our proposed method promises excellent decoupling efficiency.

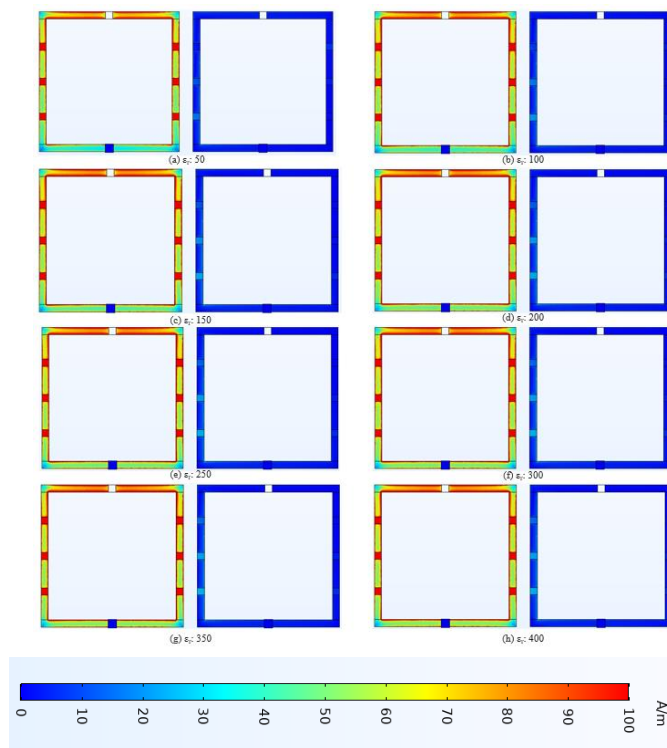


Fig. 8 Simulated current distributions of the self-decoupled coils with a dielectric sheet cover the C_{mode} capacitor where one coil is excited. The

other coil is kept as a passive element. (a) ϵ_r : 50 (b) ϵ_r : 100 (c) ϵ_r : 150 (d) ϵ_r : 200 (e) ϵ_r : 250 (f) ϵ_r : 300 (g) ϵ_r : 350 (h) ϵ_r : 400

IV. CONCLUSION AND DISCUSSION

The self-decoupled coil's high dielectric sheet significantly decreased electric fields, accounting for safer MRI at ultra-high fields. It also improved the magnetic field distribution while ensuring decoupling efficiency. In the future, Bench tests may be carried out to test our proposed method's success in a realistic setting.

Acknowledgment

This work is supported in part by the grant from NIH (U01 EB023829) and SUNY Empire Innovation Professorship Award.

REFERENCES

- [1] X. Zhang, "Novel radio frequency resonators for in vivo magnetic resonance imaging and spectroscopy at very high magnetic fields," Ph.D., Biomedical Engineering, University of Minnesota, 2002.
- [2] Z. Xie and X. Zhang, "A novel decoupling technique for non-overlapped microstrip array coil at 7T MR imaging," in *the 16th Annual Meeting of ISMRM*, Toronto, Canada, P. o. t. t. A. M. o. ISMRM, Ed., May 3 -9 2008, p. 1068.
- [3] Z. Xie and X. Zhang, "An 8-channel microstrip array coil for mouse parallel MR imaging at 7T by using magnetic wall decoupling technique," in *the 16th Annual Meeting of ISMRM*, Toronto, Canada, P. o. t. t. A. M. o. ISMRM, Ed., May 3 -9 2008, p. 2973.
- [4] Z. Xie and X. Zhang, "An 8-channel non-overlapped spinal cord array coil for 7T MR imaging," in *the 16th Annual Meeting of ISMRM*, Toronto, Canada, P. o. t. t. A. M. o. ISMRM, Ed., May 3 -9 2008, p. 2974.
- [5] Z. Xie and X. Zhang, "An eigenvalue/eigenvector analysis of decoupling methods and its application at 7T MR imaging," in *the 16th Annual Meeting of ISMRM Toronto, Canada*, Toronto, Canada, 2008, vol. 16, p. 2972.

- [6] X. Zhang, C. Wang, D. Vigneron, and S. J. Nelson, "Studies on MR Reception Efficiency and SNR of Non-resonance RF Method (NORM)," in *Proceedings of the 17th Annual Meeting of ISMRM, Honolulu, USA*, Honolulu, HI, 2009, vol. 17, p. 104.
- [7] B. Wu *et al.*, "Multi-purpose flexible transceiver array at 7T," in *Proceedings of the 17th Annual Meeting of ISMRM, Honolulu, USA*, Honolulu, HI, 2009, vol. 17, p. 107.
- [8] X. Zhang, K. Ugurbil, and W. Chen, "Method and apparatus for magnetic resonance imaging and spectroscopy using microstrip transmission line coils," (in English), Patent 7023209 Patent Appl. 09/974,184, 2006.
- [9] B. Wu *et al.*, "Flexible transceiver array for ultrahigh field human MR imaging," *Magn Reson Med*, vol. 68, no. 4, pp. 1332-8, Oct 2012. [Online]. Available: http://www.ncbi.nlm.nih.gov/entrez/query.fcgi?cmd=Retrieve&db=PubMed&dopt=Citation&list_uids=22246803
- [10] X. Yan, R. Xue, and X. Zhang, "A monopole/loop dual-tuned RF coil for ultrahigh field MRI," *Quant Imaging Med Surg*, vol. 4, no. 4, pp. 225-31, Aug 2014. [Online]. Available: http://www.ncbi.nlm.nih.gov/entrez/query.fcgi?cmd=Retrieve&db=PubMed&dopt=Citation&list_uids=25202657
- [11] Y. Pang, D. B. Vigneron, and X. Zhang, "Parallel traveling-wave MRI: a feasibility study," *Magn Reson Med*, vol. 67, no. 4, pp. 965-78, Apr 2012. [Online]. Available: http://www.ncbi.nlm.nih.gov/entrez/query.fcgi?cmd=Retrieve&db=PubMed&dopt=Citation&list_uids=21858863
- [12] Y. Pang, C. Wang, D. Vigneron, and X. Zhang, "Parallel traveling-wave MRI: antenna array approach to traveling-wave MRI for parallel transmission and acquisition," *Proceedings of the 18th Scientific Meeting and Exhibition of ISMRM*, p. 3794, 2010.
- [13] X. Yan, X. Zhang, L. Wei, and R. Xue, "Design and Test of Magnetic Wall Decoupling for Dipole Transmit/Receive Array for MR Imaging at the Ultrahigh Field of 7T," *Appl Magn Reson*, vol. 46, no. 1, pp. 59-66, Jan 2015, doi: 10.1007/s00723-014-0612-9.
- [14] X. Yan, X. Zhang, L. Wei, and R. Xue, "Magnetic wall decoupling method for monopole coil array in ultrahigh field MRI: a feasibility test," *Quant Imaging Med Surg*, vol. 4, no. 2, pp. 79-86, Apr 2014. [Online]. Available: http://www.ncbi.nlm.nih.gov/entrez/query.fcgi?cmd=Retrieve&db=PubMed&dopt=Citation&list_uids=24834419
- [15] Y. Li, Z. Xie, Y. Pang, D. Vigneron, and X. Zhang, "ICE decoupling technique for RF coil array designs," *Med Phys*, vol. 38, no. 7, pp. 4086-93, Jul 2011, doi: 10.1118/1.3598112.
- [16] X. Zhang and J. X. Ji, "Parallel and sparse MR imaging: methods and instruments-Part 1," *Quant Imaging Med Surg*, vol. 4, no. 1, pp. 1-3, Feb 2014, doi: 10.3978/j.issn.2223-4292.2014.03.01.
- [17] J. X. Ji and X. Zhang, "Parallel and sparse MR imaging: methods and instruments-Part 2," *Quant Imaging Med Surg*, vol. 4, no. 2, pp. 68-70, Apr 2014, doi: 10.3978/j.issn.2223-4292.2014.04.16.
- [18] G. Adriany *et al.*, "Transmit and receive transmission line arrays for 7 Tesla parallel imaging," *Magn Reson Med*, vol. 53, no. 2, pp. 434-45, Feb 2005. [Online]. Available: http://www.ncbi.nlm.nih.gov/entrez/query.fcgi?cmd=Retrieve&db=PubMed&dopt=Citation&list_uids=15678527
- [19] Y. Pang, X. Zhang, Z. Xie, C. Wang, and D. B. Vigneron, "Common-mode differential-mode (CMDM) method for double-nuclear MR signal

- excitation and reception at ultrahigh fields," *IEEE Trans Med Imaging*, vol. 30, no. 11, pp. 1965-73, Nov 2011. [Online]. Available: http://www.ncbi.nlm.nih.gov/entrez/query.fcgi?cmd=Retrieve&db=PubMed&dopt=Citation&list_uids=21693414
- [20] X. Zhang, C. Wang, Z. Xie, and B. Wu, "Non-resonant microstrip (NORM) RF coils: an unconventional RF solution to MR imaging and spectroscopy," in *Proceedings of International Society for Magnetic Resonance in Medicine*, Toronto, Canada, 2008, vol. 16, p. 435.
- [21] Y. Pang, E. W. Wong, B. Yu, and X. Zhang, "Design and numerical evaluation of a volume coil array for parallel MR imaging at ultrahigh fields," *Quant Imaging Med Surg*, vol. 4, no. 1, pp. 50-6, Feb 2014, doi: 10.3978/j.issn.2223-4292.2014.02.07.
- [22] Y. Pang, B. Wu, X. Jiang, D. B. Vigneron, and X. Zhang, "Tilted microstrip phased arrays with improved electromagnetic decoupling for ultrahigh-field magnetic resonance imaging," *Medicine (Baltimore)*, vol. 93, no. 28, p. e311, Dec 2014, doi: 10.1097/MD.0000000000000311.
- [23] Y. Pang, B. Yu, D. B. Vigneron, and X. Zhang, "Quadrature transmit array design using single-feed circularly polarized patch antenna for parallel transmission in MR imaging," *Quant Imaging Med Surg*, vol. 4, no. 1, pp. 11-8, Feb 2014, doi: 10.3978/j.issn.2223-4292.2014.02.03.
- [24] Y. Pang and X. Zhang, "Precompensation for mutual coupling between array elements in parallel excitation," *Quant Imaging Med Surg*, vol. 1, no. 1, pp. 4-10, Dec 2011. [Online]. Available: http://www.ncbi.nlm.nih.gov/entrez/query.fcgi?cmd=Retrieve&db=PubMed&dopt=Citation&list_uids=23243630
- [25] K. Payne, S. Khan, and X. Zhang, "Investigation of Magnetic Wall Decoupling for planar Quadrature RF Array coils using Common-Mode Differential-mode Resonators," in *Proceedings of the Annual Meeting of ISMRM 2022*, London, UK, 2022, vol. 30.
- [26] O. Rutledge, T. Kwak, P. Cao, and X. Zhang, "Design and test of a double-nuclear RF coil for (1)H MRI and (13)C MRSI at 7T," *J Magn Reson*, vol. 267, pp. 15-21, Jun 2016, doi: 10.1016/j.jmr.2016.04.001.
- [27] X. Hu, X. Chen, X. Liu, H. Zheng, Y. Li, and X. Zhang, "Parallel imaging performance investigation of an 8-channel common-mode differential-mode (CMDM) planar array for 7T MRI," *Quant Imaging Med Surg*, vol. 4, no. 1, pp. 33-42, Feb 2014. [Online]. Available: http://www.ncbi.nlm.nih.gov/entrez/query.fcgi?cmd=Retrieve&db=PubMed&dopt=Citation&list_uids=24649433
- [28] X. Yan, J. C. Gore, and W. A. Grissom, "Self-decoupled radiofrequency coils for magnetic resonance imaging," *Nat Commun*, vol. 9, no. 1, p. 3481, Aug 28 2018, doi: 10.1038/s41467-018-05585-8.
- [29] K. Payne and X. Zhang, "Hairpin Radio Frequency Coil Array with High Inter-channel isolation for 7T Magnetic Resonance Imaging," in *Proceedings of the Annual Meeting of ISMRM 2022*, 2022, vol. 30.
- [30] K. Payne, L. Ying, and X. Zhang, "Hairpin RF Resonators for Transceiver Arrays with High Inter-channel Isolation and B1 Efficiency at Ultrahigh Field 7T MR Imaging," *arXiv preprint arXiv:2201.08794*, 2022/1/21 2022, doi: arXiv:2201.08794.
- [31] N. I. Avdievich, J. W. Pan, and H. P. Hetherington, "Resonant inductive decoupling (RID) for transceiver arrays to compensate for both reactive and resistive components of the mutual impedance," *NMR Biomed*, vol. 26, no. 11, pp. 1547-54, Nov 2013, doi: 10.1002/nbm.2989.
- [32] C. Wang and X. Zhang, "Evaluation of B1+ and E field of RF Resonator with High Dielectric Insert,"

- in *Proceedings of the 17th Annual Meeting of ISMRM, Honolulu, Hawaii*, 2009, p. 3054.
- [33] W. M. Teeuwisse, W. M. Brink, K. N. Haines, and A. G. Webb, "Simulations of high permittivity materials for 7 T neuroimaging and evaluation of a new barium titanate-based dielectric," *Magn Reson Med*, vol. 67, no. 4, pp. 912-8, Apr 2012, doi: 10.1002/mrm.24176.
- [34] T. P. A. O'Reilly, A. G. Webb, and W. M. Brink, "Practical improvements in the design of high permittivity pads for dielectric shimming in neuroimaging at 7T," *J Magn Reson*, vol. 270, pp. 108-114, Sep 2016, doi: 10.1016/j.jmr.2016.07.003.
- [35] K. Haines, N. B. Smith, and A. G. Webb, "New high dielectric constant materials for tailoring the B1+ distribution at high magnetic fields," *J Magn Reson*, vol. 203, no. 2, pp. 323-7, Apr 2010, doi: 10.1016/j.jmr.2010.01.003.
- [36] J. E. Snaar *et al.*, "Improvements in high-field localized MRS of the medial temporal lobe in humans using new deformable high-dielectric materials," *NMR Biomed*, vol. 24, no. 7, pp. 873-9, Aug 2011, doi: 10.1002/nbm.1638.
- [37] W. M. Brink and A. G. Webb, "High permittivity pads reduce specific absorption rate, improve B1 homogeneity, and increase contrast-to-noise ratio for functional cardiac MRI at 3 T," *Magn Reson Med*, vol. 71, no. 4, pp. 1632-40, Apr 2014, doi: 10.1002/mrm.24778.